

1 RNA chaperones Hfq and ProQ play a key role in the virulence of the 2 plant pathogenic bacterium *Dickeya dadantii*

3
4 Simon Leonard¹, Camille Villard¹, William Nasser¹, Sylvie Reverchon^{1*}, Florence Hommais^{1*}

5 ¹ Université de Lyon, INSA-Lyon, Université Claude Bernard Lyon1, CNRS, UMR5240 MAP,
6 Microbiologie, Adaptation, Pathogénie, F-69622, Villeurbanne CEDEX, France

7
8 * Correspondence:

9 Florence Hommais, Sylvie Reverchon

10 florence.hommais@univ-lyon1.fr; Sylvie.reverchon-pescheux@insa-lyon.fr

11
12 Running title: *Dickeya dadantii proQ* and *hfq* mutant characterization

13
14 **Keywords:** *Dickeya dadantii*¹, *proQ*², *hfq*³, virulence⁴, non coding RNA⁵. (Min.5-Max. 8)

15 Abstract

16 *Dickeya dadantii* is an important pathogenic bacterium that infects a number of crops including potato
17 and chicory. While extensive works have been carried out on the control of the transcription of its
18 genes encoding the main virulence functions, little information is available on the post-transcriptional
19 regulation of these functions. We investigated the involvement of the RNA chaperones Hfq and ProQ
20 in the production of the main *D. dadantii* virulence functions. Phenotypic assays on the *hfq* and *proQ*
21 mutants showed that inactivation of *hfq* resulted in a growth defect, a modified capacity for biofilm
22 formation and strongly reduced motility, and in the production of degradative extracellular enzymes
23 (proteases, cellulase and pectate lyases). Accordingly, the *hfq* mutant failed to cause soft rot on chicory
24 leaves. The *proQ* mutant had reduced resistance to osmotic stress, reduced extracellular pectate lyase
25 activity compared to the wild-type strain, and reduced virulence on chicory leaves. Most of the
26 phenotypes of the *hfq* and *proQ* mutants were related to the low amounts of mRNA of the
27 corresponding virulence factors. Complementation of the double mutant *hfq-proQ* by each individual
28 protein and cross-complementation of each chaperone suggested that they might exert their effects via
29 partially overlapping but different sets of targets. Overall, it clearly appeared that the two Hfq and ProQ
30 RNA chaperones are important regulators of pathogenicity in *D. dadantii*. This underscores that
31 virulence genes are regulated post transcriptionally by non-coding RNAs.

32 1 Introduction

33 *Dickeya dadantii* is a Gram-negative phytopathogenic bacterium responsible for soft rot disease in a
34 wide range of plant species including economically important crops (e.g. potato, chicory, sugar beet)
35 and many ornamental plants (Ma et al., 2007). It causes important production losses (Toth et al., 2011).

Dickeya dadantii proQ and *hfq* mutant characterization

36 Virulence mechanisms of *D. dadantii* have been extensively studied (Ma et al., 2007). The infection
37 process is divided in two distinct phases: (i) an asymptomatic phase when the bacterium penetrates into
38 the host and progresses through intercellular spaces without multiplying substantially; (ii) a
39 symptomatic phase associated with strongly increased bacterial fitness and multiplication (Fagard et
40 al., 2007). Globally, the four main steps of plant infection by *Dickeya* are the following: (i) adherence
41 to the plant surface and entry into the plant tissues, via wound sites or through natural openings such
42 as stomata, (ii) colonization of the apoplastic spaces between plant cells, (iii) suppression of the host
43 defense response, and (iv) plant cell wall degradation (through degradative extracellular enzyme
44 production, mainly pectate lyases) resulting in the development of disease symptoms. Each of these
45 disease stages and life-history transitions requires the correct spatio-temporal production of the
46 different adaptive and virulence factors (including those involved in adhesion, motility, stress
47 resistance and plant cell wall degradation) in response to various signals (changes in cell density,
48 variation in environmental physico-chemical parameters, and host disease reaction) (Reverchon and
49 Nasser, 2013).

50 To characterize the regulation of this pathogenic process, investigations on *D. dadantii* have mostly
51 focused on its control by DNA-binding transcription factors (Reverchon and Nasser, 2013; Leonard et
52 al., 2017) with a few additional studies about the regulatory role of chromosome dynamics (Ouafa et
53 al., 2012; Jiang et al., 2015; Meyer et al., 2018). Knowledge of the post-transcriptional regulation of
54 virulence factor production by sRNAs in *D. dadantii* is still in its infancy.

55 Post-transcriptional regulation is defined as the control of gene expression at the RNA level and
56 classically occurs through base-pairing interactions between regulatory RNAs (sRNAs) and mRNAs.
57 This base pairing can have positive or negative effects on the stability and/or the translation of the
58 targeted mRNA. These sRNAs can be broadly divided into two categories according to their genomic
59 location: (i) *cis*-acting antisense sRNAs are transcribed from the opposite strand of their targets and
60 act via extensive base pairing; (ii) *trans*-acting sRNAs mostly originate from intergenic regions, display
61 partial sequence complementarities with their mRNA targets and can regulate more than one target.
62 The interactions between sRNAs and their targets are often assisted by specialized RNA-binding
63 proteins called RNA chaperones.

64 A prominent bacterial RNA chaperone is the Hfq protein which contributes to regulation by *trans*-
65 acting sRNAs in many bacteria (Updegrove et al., 2016). Hfq was first discovered in *Escherichia coli*
66 as an essential host factor of the RNA bacteriophage Qbeta. Hfq impacts multiple steps, like changing
67 RNA structure, bringing RNAs into proximity, neutralizing the negative charge of the two pairing
68 RNAs, stimulating the nucleation of the first base pairs as well as facilitating the further annealing of
69 the two RNA strands. While estimates of the number of Hfq vary from $\approx 20,000$ to 60,000 (Kajitani et
70 al., 1994; Ali Azam et al., 1999), it is clear that Hfq is limiting under most conditions (Wagner, 2013).

71 Other proteins with possible chaperone activity have been reported recently. For example, the
72 monomeric ProQ protein of *Salmonella enterica* is an RNA-binding protein that interacts with and
73 stabilizes over 50 highly structured antisense and *trans*-acting sRNAs. (Smirnov et al., 2016). The
74 cellular concentration of ProQ was estimated to be 2,000 copies per cell (Sheidy and Zielke, 2013).
75 This protein was originally identified as being important for osmolyte accumulation in *E. coli* by
76 increasing cellular levels of the proline transporter ProP (Milner and Wood, 1989; Kunte et al., 1999)
77 and was later shown to possess RNA strand exchange and RNA annealing activities (Chaulk et al.,
78 2011). Thus, ProQ was initially described as an RNA chaperone that controls ProP levels in *E. coli*. In
79 *Legionella pneumophila*, the ProQ equivalent protein (called RocC) interacts with one *trans*-acting
80 sRNA to control the expression of genes involved in natural transformation (Attaiech et al., 2016).

81 ProQ belongs to the RNA-binding proteins of the FinO family. FinO has been studied for its role as an
82 RNA chaperone in antisense regulation of F plasmid conjugation in *E. coli* (Mark Glover et al., 2015).
83 As shown in *S. enterica*, ProQ seems to recognize stable RNA hairpins such as transcriptional
84 terminators and reading the RNA structure rather than its sequence (Holmqvist et al., 2018).

85 While several recent studies have addressed a potential role of Hfq in the virulence of phytopathogenic
86 bacteria like *Agrobacterium tumefaciens* (Wilms et al., 2012), *Erwinia amylovora* (Zeng et al., 2013),
87 *Pectobacterium carotovorum* (Wang et al., 2018) and *Xanthomonas campestris* (Lai et al., 2018),
88 nothing is known about the impact of Hfq and ProQ on *D. dadantii* virulence. Moreover, potential links
89 between ProQ and the virulence of plant-pathogenic bacteria have never been established. To address
90 these questions, we constructed and characterized *hfq* and *proQ* mutants. Loss of Hfq or ProQ resulted
91 in drastically reduced virulence. This phenotype was associated with the alteration of several virulence
92 determinants including pectate lyase production, motility, and adhesion. Additionally, analyses of
93 mutants defective in the two proteins suggested that these two RNA chaperones might exert their
94 effects via partially overlapping but different sets of targets.

95 **2 Materials and Methods**

96 **2.1 Bacterial strains, plasmids and culture conditions**

97 The bacterial strains, plasmids, phages and primers used in this study are described in Tables S1, S2
98 and S3. *E. coli* and *D. dadantii* strains were grown at 37°C and 30°C, respectively, in Luria-Bertani
99 broth (LB) medium or in M63 minimal medium (Miller, 1972) supplemented with 0.1 mM CaCl₂,
100 0.2% (w/v) sucrose and 0.25% (w/v) polygalacturonate (PGA, a pectin derivative) as carbon sources.
101 PGA induces the synthesis of pectate lyases, which are the essential virulence factors of *D. dadantii*.
102 When required, the media were supplemented with antibiotics at the following concentrations:
103 ampicillin (Amp) 100 µg/mL, chloramphenicol (Cm) 20 µg/mL, kanamycin (Kan) 50 µg/mL. The
104 media were solidified with 1.5 % (w/v) Difco agar. Liquid cultures were grown in a shaking
105 incubator (220 r.p.m.). Bacterial growth in liquid medium was estimated by measuring turbidity at
106 600 nm (OD₆₀₀) to determine growth rates.

107 **2.2 Gene knockout and complementation of the Hfq- and ProQ-encoding genes in *D. dadantii***

108 The *hfq* gene was inactivated by introducing a *uidA-Kan* cassette into the unique *BsrGI* restriction
109 site present in its open reading frame. The *uidA-Kan* cassettes (Bardonnnet and Blanco, 1992)
110 includes a promoterless *uidA* gene that conserves its Shine Dalgarno sequence.

111 To create a Δ *proQ*::Cm mutant, segments located 500 bp upstream and 500 bp downstream of *proQ*
112 were amplified by PCR using primer pairs P1-P2 and P3-P4 (Table S3). Primers P2 and P3 included
113 a unique restriction site for *BglII* and were designed to have a short 20-bp overlap of complementary
114 sequences. The two separate PCR fragments were attached together by overlap extension polymerase
115 chain reaction using primers P1 and P4. The resulting Δ *proQ*-*BglII* PCR product was cloned into a
116 pGEMT plasmid to create plasmid pGEM-T- Δ *proQ*-*BglII*. The Cm resistance cassette from plasmid
117 pKD3 (Datsenko and Wanner, 2000) was inserted into the unique *BglII* site of pGEM-T- Δ *proQ*-*BglII*
118 to generate pGEM-T- Δ *proQ*::Cm (Table S2).

119 We took care to select cassettes without transcription termination signals in order to avoid polar
120 effects on downstream genes for both insertions. The insertions were introduced into the *D. dadantii*
121 chromosome by marker exchange recombination between the chromosomal allele and the plasmid-
122 borne mutated allele. The recombinants were selected after successive cultures in low phosphate
123 medium in the presence of the suitable antibiotic because pBR322 derivatives are very unstable in

***Dickeya dadantii proQ* and *hfq* mutant characterization**

124 these conditions (Roeder and Collmer, 1985). Correct recombination was confirmed by PCR.
125 Mutations were transduced into a clean *D. dadantii* 3937 genetic background using phage Φ EC2
126 (Table S1).

127 For complementation of the *hfq* and *proQ* mutations, the promoter and coding sequences of the *proQ*
128 and *hfq* genes were amplified from *D. dadantii* 3937 genomic DNA using primers P5/P6 and P7/P8,
129 respectively (Table S3). The forward primers (P5 and P7) included a unique restriction site for *NheI*,
130 and the reverse primers (P6 and P8) included a unique restriction site for *HindIII*. After digestion
131 with *NheI* and *HindIII*, each PCR fragment was ligated into pBBR1-mcs4 previously digested by
132 *NheI* and *HindIII* to generate pBBR1-mcs4::*hfq* and pBBR1-mcs4::*proQ*, respectively (Table S2).
133 Correct constructions were confirmed by sequencing.

134 2.3 Agar plate detection tests for pectate lyase, cellulase, protease and other enzyme assays

135 Protease activity was detected on medium containing skim milk (12.5 g L⁻¹). Cellulase activity was
136 detected on carboxymethylcellulose agar plates with the Congo red staining procedure (Teather and
137 Wood, 1982). Pectate lyases were assayed on toluenized cell extracts. Pectate lyase activity was
138 measured by recording the degradation of PGA into unsaturated products that absorb at 230 nm
139 (Moran et al., 1968). Specific activity was expressed as nmol of unsaturated products liberated per
140 min per mg of bacterial dry weight, given that an OD₆₀₀ of 1 corresponded to 10⁹ bacteria.mL⁻¹ and to
141 0.47 mg of bacterial dry weight.mL⁻¹.

142 2.4 Stress resistance assays

143 Bacteria were cultured at 30°C in 96-well plates using M63S (M63 + 0.2% w/v sucrose), pH 7.0, as
144 minimal medium. Bacterial growth (OD₆₀₀) was monitored for 48 h using an [Infinite® 200 PRO -](#)
145 [Tecan](#) instrument. Resistance to osmotic stress was analyzed using M63S enriched in 0.05 to 0.5 M
146 NaCl. Resistance to oxidative stress was analyzed in the same medium by adding H₂O₂
147 concentrations ranging from 25 to 200 μM. The pH effect was analyzed using the same M63S
148 medium buffered with malic acid at different pH values ranging from 3.7 to 7.0.

149 2.5 Biofilm measurements

150 Biofilm formation was quantified using the microtiter plate static biofilm model. Bacteria were
151 grown for 48 h at 30°C in 24-well plates in M63 medium supplemented with glycerol as the carbon
152 source. Then, the supernatant was removed, and the biofilm was washed once with 1mL of M63
153 medium and resuspended in 1 mL of the same medium. The percentage of adherence was then
154 calculated as the ratio of the number of cells in the biofilm over the total number of cells, i.e. biofilm
155 cells over planktonic cells. The amount of planktonic cells was estimated by measuring the optical
156 density at 600 nm of the supernatant and the washing buffer. The amount of cells in the biofilm was
157 estimated by measuring the OD₆₀₀ of the biofilm resuspended in M63.

158 2.6 Motility and chemotaxis assays

159 For the *proQ* mutant, motility assays were performed on semi-solid LB agar plates. An overnight
160 bacterial culture was prepared as described above, and then inoculated in the centre of each of eight
161 Petri dishes with a sterile toothpick. For motility experiments, 0.3% agar plates were used. Halo sizes
162 were examined after incubation at 30°C for 24 h. Motility indexes were calculated as the ratios of
163 the mutant halo size over the wild type (WT) halo size.

164 For the *hfq* mutant, motility assays were performed in competition (to avoid the influence of bacterial
165 growth), as previously described (Ashby et al., 1988). Briefly, 10 mL of bacteria in their exponential
166 growth phase were washed twice in sodium-free buffer and then concentrated in 3 mL. Capillary
167 assays were performed in competition in an equal 1:1 ratio. Suspension dilutions of chemotaxis
168 assays were spotted onto selective LB agar medium. Different bacterial populations were thus
169 enumerated on LB agar plates (both wild-type cells and *hfq::uidA*-Kan mutants) and LB agar plates
170 containing kanamycin (*hfq::uidA*-Kan mutants). Motility indexes were calculated as the ratios of the
171 number of *hfq::uidA*-Kan mutants over the number of wild-type cells.

172 2.7 Virulence assays

173 Virulence assays were performed on wounded chicory leaves by depositing a drop of inoculum as
174 previously described (Dellagi et al., 2005). Briefly, chicory leaves were wounded with a 2 cm
175 incision using a sterile scalpel, inoculated with 5 μ L of bacterial suspension ($OD_{600}=1$) and incubated
176 at 30°C in a dew chamber at 100% relative humidity. Disease severity was determined 18 h and 48 h
177 after inoculation by collecting and weighing the macerated tissues.

178 2.8 Quantitative RT-PCR analyses

179 Gene expression analyses were performed using qRT-PCR. Total RNAs were extracted and purified
180 from cultures grown to the late exponential phase ($OD_{600} = 0.8$) as previously described (Maes and
181 Messens, 1992; Hommais et al., 2008). Reverse transcription and quantitative PCR were performed
182 using the REvertAid First Strand cDNA synthesis kit and the Maxima SYBR Green/ROX qPCR
183 Master Mix (Thermo Scientific) with an LC480 Lightcycler (Roche). Primer specificity was verified
184 by melting curve analysis. qPCR primers are listed in Table S4.

185 2.9 Data representation and statistical analysis

186 Boxplot representations were generated using R software (R Core Team, 2020) and the beeswarm
187 package (Eklund, 2016). Statistical analysis was performed using Wilcoxon Mann-Whitney tests, and
188 differences were considered significant when the p value < 0.05 .

189 3 Results

190 3.1 Analysis of *D. dadantii* Hfq and ProQ protein sequences and their genomic contexts

191 *E. coli* and *D. dadantii* Hfq proteins displayed 83% identity. The highest identity level was in the N-
192 terminal region (amino acids 1-74), which forms the core of the protein and contains its RNA-
193 binding sites (Link et al., 2009). Most of the amino acids involved in RNA interactions were
194 conserved except E18, which was K18 in *D. dadantii* (Figure S1). *D. dadantii* ProQ was 68%
195 identical with *E. coli* ProQ, with also high identity in the N-terminal FinO domain of ProQ, which is
196 the primary determinant of its RNA-binding capacity (Chaulk et al., 2011; Gonzalez et al., 2017). In
197 particular, the regions spanning residues 1-10 and 92-105, shown to interact with RNA, were highly
198 conserved (Gonzalez et al., 2017). All the residues involved in the formation of a basic patch on the
199 protein surface (R32, R69, R80, R100, K101, K107, and R114) – an important structure for
200 interaction with RNAs – were conserved (Figure S1).

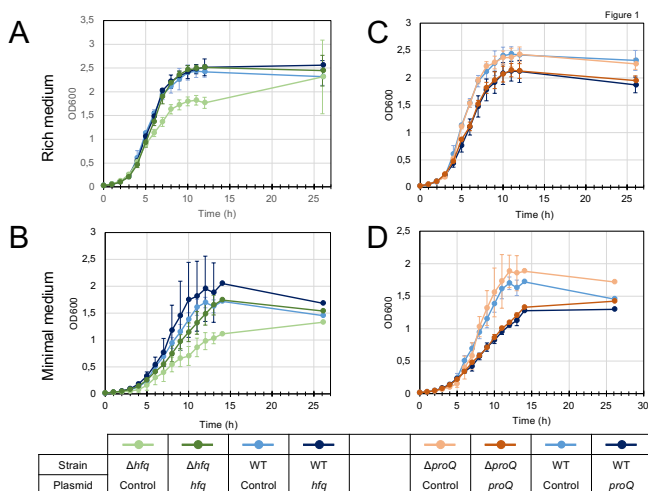
201 The *hfq* and *proQ* genes are embedded in the same chromosomal context in *D. dadantii* as in other
202 bacteria such as *E. coli* or *S. enterica* (Figure S2). The *hfq* gene is part of the well conserved *amiB*-
203 *mutL-miaA-hfq-hflXKC* cluster (Tsui and Winkler, 1994), while *proQ* is localized between *yebR* and
204 *prc*. Inspection of the transcriptomes of *D. dadantii* under various physiological conditions

Dickeya dadantii *proQ* and *hfq* mutant characterization

205 (Reverchon et al., 2021) showed that transcription of *hfq* could be driven by (i) a promoter upstream
 206 of *mutL*, (ii) a promoter inside *mutL* and upstream of *miaA*, or (iii) two promoters inside *miaA*
 207 and upstream of *hfq* (Figure S2). Considering the expression level of *mutL-miaA-hfq* genes, it appears
 208 that *hfq* was largely transcribed from the two promoters inside *miaA* and rarely co-transcribed with
 209 *miaA*. The downstream genes showed similar expression profiles and did not exhibit any promoter
 210 activity downstream of *hfq*, suggesting that they may be co-transcribed with *hfq* in the same way as
 211 in *E. coli* (RegulonDB, <http://regulondb.ccg.unam.mx/>). Two promoters were found upstream of the
 212 *proQ* gene (one between *proQ* and *yebR* and one upstream of *yebR*) (Figure S2B). Regarding the
 213 difference in read coverage obtained from RNA-seq experiments, *yebR* and *proQ* seemed to be
 214 largely transcribed separately (Figure S2B). On the contrary, *prc* and *proQ* had similar coverage, and
 215 no transcription start site was found between them, supporting co-transcription similarly to what is
 216 observed in *E. coli* (RegulonDB, <http://regulondb.ccg.unam.mx/>).

217 3.2 Phenotypic characterization of the *hfq* and *proQ* mutants

218 We first analyzed the growth characteristics of the *hfq* and *proQ* mutants. The WT, *hfq* and *proQ*
 219 strains were grown in LB rich medium and in M63 minimal medium supplemented with sucrose as
 220 the sole carbon source. While the *proQ* mutant and the WT grew similarly in both media, the *hfq*
 221 mutant exhibited delayed growth. However, in rich medium both the WT strain and *hfq* mutant
 222 reached the same optical density after being grown for 26 hrs (Figure 1A). In minimal medium with
 223 sucrose as the sole carbon source, the *hfq* mutant grew much more slowly than the WT, and reached
 224 the stationary phase at a lower optical density (Figure 1B). The growth defect of the *hfq* mutant was
 225 fully restored by complementation with plasmid pBBR-mcs4::*hfq* (Figure 1), indicating that the
 226 *hfq*::*uidA*-Kan insertion had no polar effects on downstream *hflXKC* genes. In contrast,
 227 transformation of the *proQ* mutant and WT strains with the pBBR-mcs4::*proQ* plasmid expressing
 228 *proQ* led to a lower growth rate, especially in minimal medium (Figure 1D). The two strains grew
 229 similarly in the absence of the pBBR-mcs4::*proQ* plasmid. This suggests that slight ProQ
 230 overexpression compromises growth irrespective of the genetic background. These data demonstrate
 231 that *hfq* mutation retards cellular growth, while *proQ* mutation does not. The effect was more
 232 pronounced in minimal medium compared to rich medium, suggesting that Hfq plays a more
 233 important role in the ability of *D. dadantii* to grow under conditions of nutrient limitation. A similar
 234 growth defect of *hfq* mutants has been observed in other bacteria such as *P. carotovorum* (Wang et al.,
 235 2018), *A. tumefaciens* (Wilms et al., 2012) or *E. amylovora* (Zeng et al., 2013).



236

237 **Figure 1: Growth of the wild type, mutant and complemented strains in LB rich medium (A and C) and M63**
238 **minimal medium supplemented with sucrose (B and D). Overnight bacterial precultures were diluted to an OD₆₀₀**
239 **of 0.03 in the same growth medium. OD₆₀₀ measurements of the culture were made at regular intervals to**
240 **determine growth rates. The experiment was repeated three times. The graph shows curves from one**
241 **representative experiment.**

242

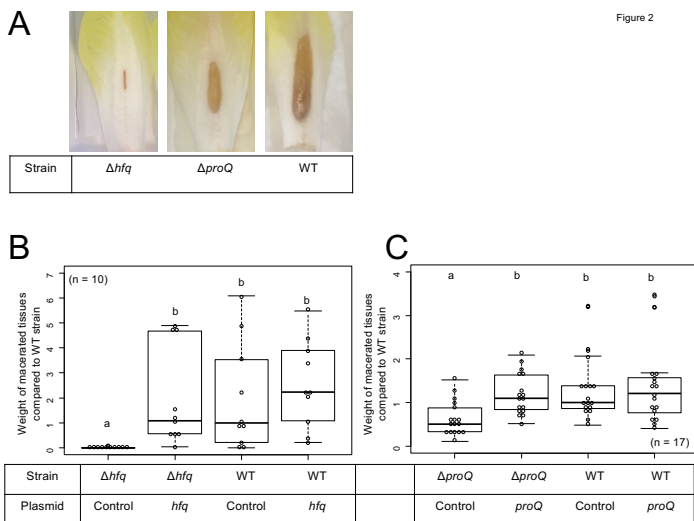
243 *Dickeya* encounter various stresses during their pathogenic growth, so we assessed the stress
244 resistance of the *hfq* and *proQ* mutants (Figure S3). They both showed behaviors similar to the WT
245 strain regarding pH and H₂O₂ stress resistance, but displayed a higher sensitivity to osmotic stress
246 than the WT strain did. The *hfq* mutant displayed a 50% growth rate reduction on 0.4 M NaCl, while
247 the WT strain was only slightly affected (20% growth rate reduction). This effect was even more
248 pronounced at 0.5 M NaCl, with a growth rate reduction of 90 % for *hfq* compared to 60% for the
249 WT. The *proQ* mutant did not grow at 0.3M NaCl and at higher NaCl concentrations (Figure S3).
250 Complementation experiments revealed that expression of *hfq* or *proQ* from an episome (plasmid
251 pBBR-mcs4::*hfq* and pBBR1-mcs4::*proQ*) fully restored the osmotic resistance of the two mutants to
252 the WT level (Figure S3). We inferred that the two chaperones are involved in providing resistance to
253 osmotic stress. Overall, this result is consistent but not identical with previous studies showing that
254 Hfq and ProQ contribute to stress tolerance, including nutrient deprivation, osmotic stress and
255 oxidative stress in *Salmonella* and *E. coli* (Chaulk et al., 2011; Smirnov et al., 2017).

256 **3.3 Hfq and ProQ are required for full virulence of *Dickeya dadantii***

257 The virulence of the *hfq* and *proQ* mutants was tested on chicory leaves. The *hfq* mutant was severely
258 impaired in virulence, and soft rot symptoms were drastically reduced (Figure 2A). Disease
259 symptoms were observed following inoculation with the *proQ* mutant and the WT strain, but they
260 were less severe in the *proQ* background. Quantitative results obtained by measuring the weight of
261 macerated tissues showed a significant difference between the disease symptoms induced by each
262 strain (p-value = 1.5e-3) (Figure 2B & C). As observed previously, the virulence defect of the *hfq*
263 mutant was more severe than that of the *proQ* mutant, in as far as the *hfq* mutant did not exhibit any
264 macerated tissue (p-value = 5.7e-4). Consequently, we did not weigh any macerated tissue in the *hfq*
265 mutant. The soft rot symptoms caused by the *hfq* and *proQ* mutants did not increase over longer
266 incubation times (48 h). The lower virulence of *hfq* and *proQ* was therefore not solely related to
267 retarded cellular growth. Complementation experiments revealed that expression of *hfq* from an
268 episome (plasmid pBBR-mcs4::*hfq*) fully restored the impaired virulence of the *hfq* mutant (Figure
269 2B). Likewise, expression of *proQ* from an episome (plasmid pBBR-mcs4::*proQ*) restored the
270 impaired virulence of the *proQ* mutant (Figure 2C).

271 Thus, the *hfq* and *proQ* genes are required for efficient pathogenic growth since both mutants were
272 clearly impaired in initiating maceration and inducing soft rot symptoms, albeit to different extents.

Dickeya dadantii *proQ* and *hfq* mutant characterization



273

274 **Figure 2: Impact of Hfq and ProQ on *D. dadantii* virulence. A, Representative examples of symptoms induced by**
 275 **the wild type and mutant strains; B and C, weights of macerated tissues following infection by the *hfq* and *proQ***
 276 **mutants, the wild type strain and the complemented strains. Data were normalized based on the weights of**
 277 **macerated tissues from the wild-type strain. Chicory leaf assays were performed as described in the Materials and**
 278 **methods section with an incubation time of 18h, and weights of macerated tissues were measured. a/b/c/d boxplot**
 279 **annotations highlight significant differences ($P < 0.05$, Wilcoxon Mann-Whitney test).**

280

281 **3.4 Production of late virulence factors, pectate lyase, protease and cellulase, is abolished in** 282 **the *hfq* mutant and reduced in the *proQ* mutant**

283 *D. dadantii* is known to use several essential virulence factors that collectively contribute to its
 284 ability to cause disease. These factors include production of cell-wall-degrading enzymes like pectate
 285 lyases, proteases and cellulase, which are responsible for soft rot symptoms. To clarify whether Hfq
 286 and ProQ have any influence on the production of key virulence factors, we compared enzyme
 287 activity in *hfq* and *proQ* mutant extracts with WT strain extracts (Figure 3A). Pectate lyase activity
 288 was abolished in the *hfq* mutant (p -value = $2.4e-7$). This defect in pectate lyase activity was not a
 289 consequence of the growth defect of the *hfq* mutant since activities were normalized to cell density.
 290 Also, the levels of pectate lyase activity were significantly reduced in the *proQ* mutant compared to
 291 the WT (p -value = $2.0e-9$) (Figure 3A). Reduced cellulase and protease activities were also observed
 292 on carboxymethylcellulose and skim milk agar plates for each mutant (Figure 3B). Complementation
 293 experiments showed that the impaired production of cell-wall-degrading enzymes was restored in *hfq*
 294 and *proQ* mutant cells transformed with the pBBR-mcs4::*hfq* and pBBR-mcs4::*proQ* plasmids,
 295 respectively (Figure 3). Therefore, the impaired pathogenicity of *D. dadantii* due to *hfq* and *proQ*
 296 mutations is linked with reduced production of late virulence factors in these mutant strains.

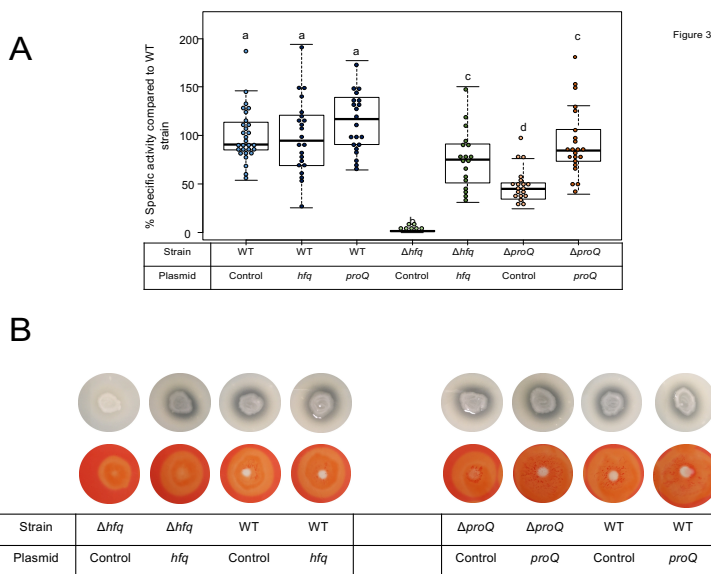


Figure 3

297

298 **Figure 3: Impact of Hfq and ProQ on cell-wall-degrading enzymes. A, Pectate lyase activity in the wild type,**
 299 **mutant and complemented strains, expressed as percent of wild type strain specific activity. a/b boxplot**
 300 **annotations highlight significant differences ($P < 0.05$, Wilcoxon Mann-Whitney test). B, protease production on**
 301 **medium containing skim milk, and cellulase production on carboxymethylcellulose agar plate with Congo red**
 302 **staining in the *hfq* and *proQ* mutants, the complemented strains and the wild type strain.**

303

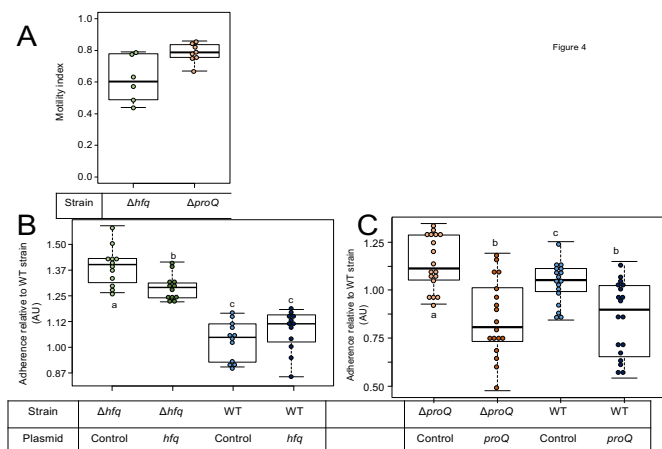
304 **3.5 Early virulence determinants such as biofilm production and motility are also impaired in** 305 **the *hfq* and *proQ* mutants**

306 At the initial stage of infection, *D. dadantii* must adhere to the plant surface and enter into the
 307 apoplast. *D. dadantii* produces cellulose fibrils, which enable it to develop aggregates on the plant
 308 surface (Jahn et al., 2011; Prigent-Combaret et al., 2012). These aggregates are embedded in an
 309 extracellular polymeric substance (EPS) that maintains a hydrated surface around the bacteria and
 310 thus helps them to survive under conditions of desiccation (Condemine et al., 1999). Motility and
 311 chemotaxis are essential for *D. dadantii* when searching for favorable sites to enter into the plant
 312 apoplast. Therefore, we evaluated the consequences of the *hfq* or *proQ* mutations on motility and
 313 biofilm formation. The ability of the *hfq* and *proQ* mutants to swim was analyzed using capillary and
 314 soft agar assays, respectively. Incubation time during the capillary assays was short, so that we were
 315 able to overlook the impact of the growth defect between the *hfq* mutant and the WT strain. Soft agar
 316 assays were performed to test the motility of the *proQ* mutant, since similar growth rates were
 317 obtained for the *proQ* mutant and the WT strain. A motility index was calculated for both
 318 experiments (Figure 4A). It was equal to the motility of the mutant strain (number of cells in the
 319 capillary or size of the halo) divided by that of the WT strain. Both *hfq* and *proQ* showed reduced
 320 motility compared to the WT (38% and -22%, respectively). This reduced cell motility is in
 321 agreement with the behavior of *hfq* mutants of most pathogenic bacteria (Chao and Vogel, 2010;
 322 Vogel and Luisi, 2011; Sobrero and Valverde, 2012; Wagner, 2013; Updegrave et al., 2016).

323 Flagellar motility negatively affects biofilm formation. Consequently, we monitored the
 324 consequences of the *hfq* or *proQ* mutations on the attachment of *D. dadantii* to the plastic coating of
 325 the microtiter plate well. From a metabolic point of view, biofilm formation reflects the trade-off
 326 between motility and exopolysaccharide (EPS) production. This trade-off was clearly unbalanced in

Dickeya dadantii *proQ* and *hfq* mutant characterization

327 favor of EPS production in the *hfq* mutant (p -value = $7.4e-7$) and less severely so in the *proQ* mutant
 328 (p -value = $3.8e-2$) (Figure 4B & C). Complementation experiments demonstrated that *hfq* expressed
 329 from an episome did not significantly reduce the increased biofilm forming capacity of the *hfq*
 330 mutant (Figure 4B). In contrast, expression of episomal *proQ* slightly decreased the biofilm
 331 formation capacity of the *proQ* mutant and WT strain (Figure 4C). These data suggest that the two
 332 RNA chaperones play different roles in *D. dadantii* biofilm formation.



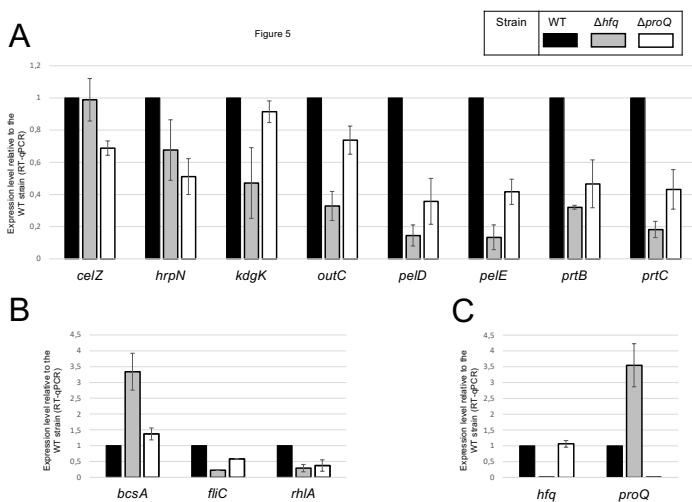
333

334 **Figure 4: Impact of Hfq and ProQ on motility and biofilm formation.** A, Motility indexes of the *hfq* and *proQ*
 335 mutants. Motility experiments were performed in capillary assays for the *hfq* mutant and in soft agar plates for
 336 the *proQ* mutant. The motility index was equal to the motility results of the mutant strain (number of cells in the
 337 capillary or halo size) divided by the results of the WT strain. B and C, impact of the *hfq* and *proQ* mutations on
 338 biofilm formation. Assays were carried out in multi-well plates. Data were normalized relative to the adherence of
 339 the wild-type strain. The effect of heterologous complementation is also showed. Quantification of the cells present
 340 in the aggregates and in the planktonic fractions for the different strains; a/b boxplot annotations highlight
 341 significant differences ($P < 0.05$, Wilcoxon Mann-Whitney test).

342 3.6 Transcripts of late virulence factors and early virulence determinants are impaired in the 343 *hfq* and *proQ* mutants.

344 Hfq and ProQ act post-transcriptionally, so we evaluated the mRNA amounts of various virulence
 345 genes in the *hfq* and *proQ* mutants by qRT-PCR. For genes mostly involved in the early stage of
 346 infection, we selected *fliC* which encodes flagellin, *rhIA* whose product is involved in the synthesis
 347 of a biosurfactant for swarming motility, and *bcsA* which encodes a protein involved in the
 348 production of cellulose fibrils important for adherence. Concerning late virulence genes, we retained
 349 *pelD* and *pelE* that encode pectate lyases, *priB* and *priC* that encode metalloproteases, *celZ* that
 350 encodes a cellulase, *outC* that encodes a compound of the type II secretion system which secretes
 351 pectinases and cellulase, *kdgK* that encodes the KDG kinase involved in the catabolism of
 352 polygalacturonate, and *hrpN* that encodes harpin which elicits the hypersensitive response. In line
 353 with the observed phenotypes, the RNA amounts of most genes were reduced in both mutants, much
 354 more drastically so in the *hfq* mutant than in the *proQ* mutant (Figure 5). The greater adherence of the
 355 *hfq* mutant was also correlated with the higher *bcsA* RNA amounts compared to the WT. However,
 356 *celZ* RNA amounts were similar in the *hfq* mutant and in the WT. Therefore, the reduced cellulase
 357 activity was not dependent on the *celZ* RNA amount but it could be partially due to reduced cellulase

358 secretion because the *outC* RNA amount was low in the *hfq* mutant, or to decreased CelZ translation.
359 In the *proQ* mutant, the amount of *celZ* transcripts was reduced, but the amount of *outC* transcripts
360 was not. Taken together, these results indicate that most of the observed phenotypes were correlated
361 to a decrease in the mRNA amounts from virulence genes.



362

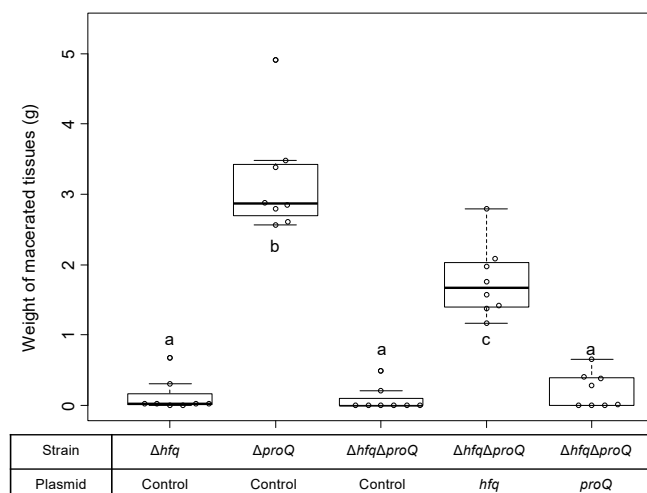
363 **Figure 5: RNA amounts in the *hfq* and *proQ* mutant strains. Gene expression levels relative to the WT strain were**
364 **evaluated in the two mutants by RT-qPCR. A, Genes encoding late virulence factors or associated with late**
365 **virulence factors; B, Genes encoding early virulence factors such as adherence and motility factors; C, Expression**
366 **levels of *hfq* and *proQ* were measured in the different mutants.**

367

368 3.7 The effects of RNA chaperones on virulence partially overlap

369 The absence of Hfq or ProQ impaired virulence and modified the production of similar virulence
370 factors. Consequently, we evaluated the behavior of a mutant inactivated for both *hfq* and *proQ* and
371 assessed whether *hfq* and *proQ* could restore virulence in the double mutant. The virulence of the *hfq*
372 *proQ* double mutant and mutant complemented by either *hfq* or *proQ* was tested on chicory leaves.
373 The mutants were asymptomatic whatever the complementation 24 h post infection, except the
374 mutant *proQ*, that caused reduced soft rot symptoms as noticed earlier (Figure 2). However, 48 h post
375 infection, the *proQ* gene inserted in the *hfq proQ* mutant produced a weight of macerated tissues
376 similar to the weight observed with the *hfq* mutant, whereas *hfq* complementation of the double
377 mutant only slightly restored soft rot symptoms (Figure 6).

Dickeya dadantii *proQ* and *hfq* mutant characterization

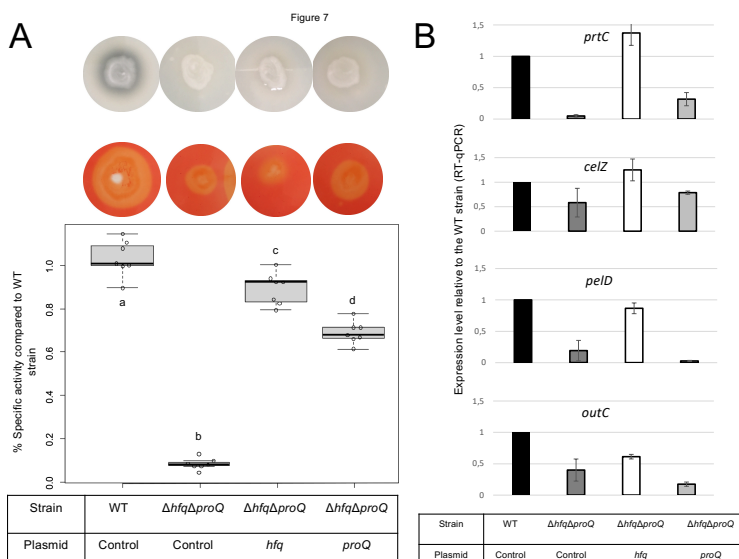


378

379 **Figure 6: *D. dadantii* virulence assays 48h post infection. Virulence was evaluated on the single mutants, the**
380 **double mutant, and the double mutant complemented by Hfq or ProQ. Chicory leaf assays were performed as**
381 **described in the Materials and methods section with an incubation time of 48h, and the weights of macerated**
382 **tissues were measured.**

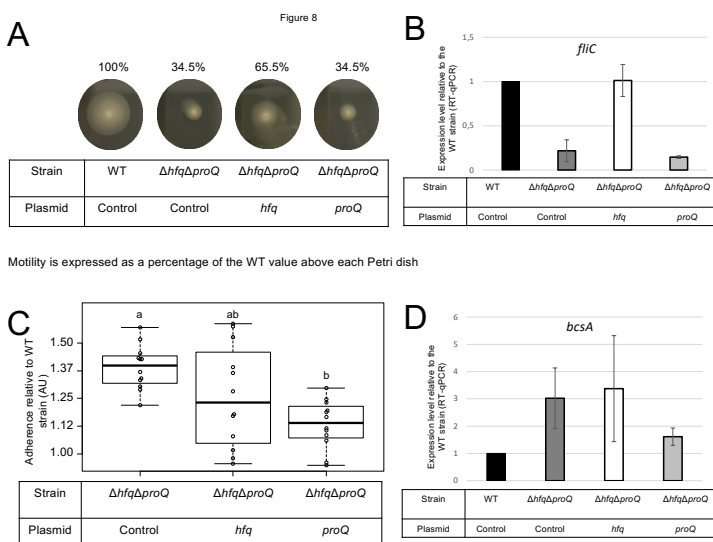
383 Late and early virulence factors were also impaired in the double mutant, as expected. Compared to
384 the *hfq* mutant, the double mutant showed a similar, perhaps higher reduction of protease, cellulase and
385 pectinase activities (Figure 7A). Motility was also reduced, and adherence was increased compared to
386 the WT (Figure 8A and C). In line with these phenotypes, the expression levels of the corresponding
387 genes were modified: *prtC*, *pelD* and *fliC* RNA amounts decreased by at least 5 folds in the double
388 mutant, and *hrpN*, *celZ* and *outC* RNA amounts decreased by about 2 folds (Figures 7B, 8 and S4).
389 Overall, the expression levels of *outC*, *pelD*, *bcsA* and *fliC* were similar in the double mutant and in
390 the *hfq* mutant, whereas the expression levels of *prtC*, *celZ* and *hrpN* decreased more than in the *hfq*
391 mutant (Figures 7B, 8B and S4).

392 The protease, pectinase and motility phenotypes were restored by complementation with Hfq.
393 Accordingly, *prtC*, *pelD* and *fliC* RNA amounts increased significantly in the double mutant strain
394 complemented by Hfq (Figures 7B and 8B). However, the cellulase phenotype was not complemented
395 by the addition of Hfq, even if the expression level of *celZ* was restored to a level similar to those
396 measured in the WT or the *hfq* mutant (Figure 7). The adherence phenotype and the expression level
397 of *bcsA* were not complemented by an *hfq* gene expressed from a plasmid (Figure 8). ProQ
398 complementation restored protease, cellulase and pectinase activities and adherence, but not motility.
399 In accordance, the expression level of *fliC* was similar to the levels in the double mutant (Figure 8B),
400 but the expression levels of *bcsA*, *prtC*, *celZ* and *hrpN* increased in the complemented strain compared
401 to the non-complemented double mutant (Figures 7, 8 and S4). Interestingly, the expression levels of
402 genes *outC* and *pelD* were unexpectedly similar to those observed in the double mutant although
403 phenotypes were restored.



404

405 **Figure 7: Impact of the double mutant on early virulence factors. Phenotypes and expression levels were analyzed**
 406 **in the double mutant strain and the double mutant strain complemented by Hfq or ProQ. a/b/c/d boxplot**
 407 **annotations highlight significant differences ($P < 0.05$, Wilcoxon Mann-Whitney test). A, Motility was evaluated**
 408 **on semi-solid LB agar plates; B and D, Expression levels of genes were measured by RT-qPCR and compared with**
 409 **the wild type; C, Adherence was evaluated and compared with the wild-type strain.**



410

411 **Figure 8: Impact of the double mutant on early virulence factors. Phenotypes and expression levels were analyzed**
 412 **in the double mutant strain and the double mutant strain complemented by Hfq or ProQ. A, Motility was**
 413 **evaluated on semi-solid LB agar plates; B and D, Expression levels of genes were measured by RT-qPCR and**
 414 **compared with the wild type; C, Adherence was evaluated and compared with the wild-type strain. a/b boxplot**
 415 **annotations highlight significant differences ($P < 0.05$, Wilcoxon Mann-Whitney test).**

416 We measured the expression levels of *hfq* and *proQ* in the different mutants. As expected, *hfq* and
 417 *proQ* expression was not detected in the respective mutant strains or in the double mutant, but a 3-fold
 418 increase was observed for the gene expressed from the plasmid. *proQ* expression level increased in the
 419 strains defective in Hfq production, i.e. 3.5 fold in the single *hfq* mutant and around 12 fold in the

Dickeya dadantii proQ and *hfq* mutant characterization

420 double mutant complemented by *proQ*. These results can be explained by an additive effect of the *hfq*
421 mutation and of *proQ* overexpression from the plasmid (Figure 1 and S4).

422 Overall, virulence assays, phenotypes and expression level measurements suggest that the two RNA
423 chaperones Hfq and ProQ exert their effects via partially overlapping but different sets of targets.

424 4 Discussion

425 We investigated the influence of the two RNA chaperones Hfq and ProQ on the virulence of the
426 bacterial plant pathogen *D. dadantii*. Inactivation of the genes encoding these two chaperones led to
427 lower production of cell-degrading enzymes acting as major virulence factors during *D. dadantii*
428 pathogenic growth, and accordingly lower pathogenicity. Furthermore, both mutations altered
429 osmotic stress tolerance and cell motility. However, the same mutations elicited different effects on
430 cell growth and biofilm formation. Phenotypes were mostly correlated with altered expression of
431 genes encoding virulence factors (*hrpN*, *outC*, *pelD*, *pelE prtC*, *prtB*), motility components (*fliC* and
432 *rhlA*) and adherence components (*bcsA*), except *celZ* expression in the *hfq* mutant. Expression levels
433 generally decreased less following inactivation of *proQ* than following inactivation of *hfq*, but both
434 RNA chaperones affected similar virulence factors. So far, the involvement of ProQ in virulence has
435 been only reported in *Salmonella* where it regulates motility directly by downregulating *fliC* mRNA
436 and represses or activates the expression of virulence genes (genes localized in SPI and SPII,
437 respectively). Accordingly, infection by a *Salmonella proQ* mutant resulted in a decreased invasion
438 rate in eukaryotic cells (Westermann et al., 2019). The present study reports for the first time the
439 involvement of ProQ in the virulence of a plant-pathogenic bacterium. In *D. dadantii*, the amount of
440 *fliC* mRNA decreased in the *proQ* mutant, but major virulence genes (*pel*, *prt* and *cel*) were repressed
441 by ProQ. Differences in *proQ* mutant behavior were also highlighted by comparing mutant strains in
442 *E. coli* and *D. dadantii*: the *proQ* mutant displayed impaired biofilm formation in *E. coli*, whereas it
443 displayed increased adherence in *D. dadantii* (Sheidy and Zielke, 2013). Overall, this illustrates the
444 species specificities of the ProQ regulatory networks, as previously described (Attaiech et al., 2016;
445 Holmqvist et al., 2018; Smirnov et al., 2016; Westermann et al., 2019). Specificities could be a
446 consequence of a rather distinct sRNA landscape produced by these bacterial species, where only
447 small numbers of sRNA homologs overlap (Leonard et al., 2019). In contrast to ProQ, Hfq proteins
448 have already been reported to significantly reduce virulence in several plant-pathogenic bacteria like
449 *A. tumefaciens*, *E. amylovora* and *P. carotovorum*. However, the role of Hfq still remains only
450 partially understood (Wilms et al., 2012) Zeng et al., 2013; Wang et al., 2018). The phenotypes of the
451 *D. dadantii hfq* mutant are similar to those of the *P. carotovorum hfq* mutant: *hfq*-defective strains
452 present a decreased growth rate, low cellulase, protease and pectinase production, and altered biofilm
453 formation and motility.

454 One interesting feature highlighted by this study is the interplay between the two RNA chaperones.
455 The mitigated virulence of the double mutant was only slightly complemented by Hfq or ProQ, so we
456 evaluated the ability of Hfq and ProQ to cross-complement each other regarding mitigation of
457 virulence. ProQ partially complemented the *hfq* mutant, whereas episomal *hfq* did not complement
458 the *proQ* mutant (Figure S5). Overall, these results indicate that these two RNA chaperones might
459 exert their effects via partially overlapping but different sets of targets. Although first reports indicate
460 that the RNAs bound by ProQ generally differ from those bound by Hfq (Holmqvist et al., 2018),
461 recent studies have demonstrated an unexpected overlap of the sets of Hfq and ProQ targets in
462 *Salmonella* and *E. coli*, with 30% of overlapping interactions (Westermann et al., 2019; Melamed et
463 al., 2020). In line with these results, we identified potential ProQ-specific targets such as *celZ*, but
464 also overlapping targets – the *fliC*, *bcsA*, *pel* and *prt* genes. Nonetheless, the expression of the target
465 genes was more highly impacted in the double mutant than in each single mutant, indicating putative

466 additive effects of the two proteins. Additionally, analyses of the expression levels of these target
467 genes in the double mutant complemented by each protein highlighted 3 classes of genes: (i) *hrpN*-
468 like genes, whose expression level is restored by Hfq or ProQ, (ii) genes whose expression levels are
469 restored at least partially only by Hfq (e.g. *fliC*, *priC*, *outC* and *pelE*), and (iii) genes whose
470 expression levels are partially restored only by ProQ (e.g. *bcsA*). Although further studies aimed at
471 identifying the direct targets of Hfq and ProQ in *D. dadantii* by *in vivo* crosslinking will clarify
472 whether the virulence functions governed by ProQ represent a subset of those governed by Hfq, these
473 data reinforce the assumption that the two proteins could have independent competing or
474 complementary roles. ProQ and Hfq could be involved in different regulatory cascades, with
475 branches converging at identical targets. Alternatively, both proteins could interact with a same
476 mRNA. The site of interaction would not necessarily be identical: ProQ recognizes its targets in a
477 sequence-independent manner, through RNA structural motifs found in sRNAs and internal to the
478 coding sequence region or at the 3' end of mRNAs (Holmqvist et al., 2018); whereas Hfq interacts
479 with nascent transcripts in the 5'-UTR of the target RNA (Kambara et al., 2018). However, the two
480 proteins could outcompete each other at a given terminator since they both have the propensity to
481 bind intrinsic terminators of RNAs (Holmqvist et al., 2016).

482 Finally, it is noteworthy that an increased level of *proQ* was measured in the *hfq* mutant and in the
483 double mutant complemented by ProQ. This is of importance because the impact of ProQ on growth
484 and biofilm production is known to be highly dependent on the amount of ProQ protein produced in
485 the cells. Taken together, these results indicate that in addition to the overlapping, complementary,
486 competing or even additive roles of these two RNA chaperones, Hfq could indirectly or directly
487 regulate ProQ production. Further analyses of the complex regulatory network of Hfq and ProQ
488 should take this possible regulation into account.

489 **5 Conflict of Interest**

490 The authors declare no conflicting interest.

491 The authors declare that the research was conducted in the absence of any commercial or financial
492 relationships that could be construed as a potential conflict of interest.

493 **6 Funding**

494 This work was supported by the ANR Combicontrol grant (ANR-15-CE21-0003-01), and by a
495 grant from the FR BioEnviS.

496 **7 Acknowledgments**

497 S. Leonard received a doctoral grant from the French Ministère de l'Éducation nationale de
498 l'Enseignement Supérieur, de la Recherche et de l'innovation. The authors thank Carlos Blanco for
499 providing the *hfq* mutant, Pauline Héritier for helpful technical assistance and Georgi Muskhelishvili
500 for helpful discussion. The authors also thank Annie Buchwalter for her careful correction of English
501 language.

502 **8 References**

503 Ali Azam, T., Iwata, A., Nishimura, A., Ueda, S., and Ishihama, A. (1999). Growth phase-dependent variation
504 in protein composition of the Escherichia coli nucleoid. *J. Bacteriol.* 181, 6361–6370.

***Dickeya dadantii proQ* and *hfq* mutant characterization**

- 505 Ashby, A. M., Watson, M. D., Loake, G. J., and Shaw, C. H. (1988). Ti plasmid-specified chemotaxis of
506 *Agrobacterium tumefaciens* C58C1 toward vir-inducing phenolic compounds and soluble factors from
507 monocotyledonous and dicotyledonous plants. *J. Bacteriol.* 170, 4181–4187.
- 508 Attaiech, L., Boughammoura, A., Brochier-Armanet, C., Allatif, O., Peillard-Fiorente, F., Edwards, R. A., et
509 al. (2016). Silencing of natural transformation by an RNA chaperone and a multitarget small RNA. *Proc. Natl.*
510 *Acad. Sci. U.S.A.* 113, 8813–8818. doi:10.1073/pnas.1601626113.
- 511 Bardonnnet, N., and Blanco, C. (1992). 'uidA-antibiotic-resistance cassettes for insertion mutagenesis, gene
512 fusions and genetic constructions. *FEMS Microbiol. Lett.* 72, 243–247.
- 513 Chao, Y., and Vogel, J. (2010). The role of Hfq in bacterial pathogens. *Curr. Opin. Microbiol.* 13, 24–33.
514 doi:10.1016/j.mib.2010.01.001.
- 515 Chaulk, S. G., Smith Friedday, M. N., Arthur, D. C., Culham, D. E., Edwards, R. A., Soo, P., et al. (2011).
516 ProQ is an RNA chaperone that controls ProP levels in *Escherichia coli*. *Biochemistry* 50, 3095–3106.
517 doi:10.1021/bi101683a.
- 518 Condemine, G., Castillo, A., Passeri, F., and Enard, C. (1999). The PecT Repressor Coregulates Synthesis of
519 Exopolysaccharides and Virulence Factors in *Erwinia chrysanthemi*. *Molecular Plant-Microbe Interactions*
520 12, 45–52. doi:10.1094/MPMI.1999.12.1.45.
- 521 Datsenko, K. A., and Wanner, B. L. (2000). One-step inactivation of chromosomal genes in *Escherichia coli*
522 K-12 using PCR products. *Proc. Natl. Acad. Sci. U.S.A.* 97, 6640–6645. doi:10.1073/pnas.120163297.
- 523 Dellagi, A., Rigault, M., Segond, D., Roux, C., Kraepiel, Y., Cellier, F., et al. (2005). Siderophore-mediated
524 upregulation of Arabidopsis ferritin expression in response to *Erwinia chrysanthemi* infection. *Plant J.* 43,
525 262–272. doi:10.1111/j.1365-313X.2005.02451.x.
- 526 Eklund, A. (2016). beeswarm: The Bee Swarm Plot, an Alternative to Stripchart. R package version 0.2.3.
527 <https://CRAN.R-project.org/package=beeswarm>
- 528 Fagard, M., Dellagi, A., Roux, C., Périno, C., Rigault, M., Boucher, V., et al. (2007). *Arabidopsis thaliana*
529 expresses multiple lines of defense to counterattack *Erwinia chrysanthemi*. *Mol. Plant Microbe Interact.* 20,
530 794–805. doi:10.1094/MPMI-20-7-0794.
- 531 Gonzalez, G. M., Hardwick, S. W., Maslen, S. L., Skehel, J. M., Holmqvist, E., Vogel, J., et al. (2017).
532 Structure of the *Escherichia coli* ProQ RNA-binding protein. *RNA* 23, 696–711. doi:10.1261/rna.060343.116.
- 533 Holmqvist, E., Li, L., Bischler, T., Barquist, L., and Vogel, J. (2018). Global Maps of ProQ Binding In Vivo
534 Reveal Target Recognition via RNA Structure and Stability Control at mRNA 3' Ends. *Mol. Cell* 70, 971-
535 982.e6. doi:10.1016/j.molcel.2018.04.017.
- 536 Holmqvist, E., Wright, P. R., Li, L., Bischler, T., Barquist, L., Reinhardt, R., et al. (2016). Global RNA
537 recognition patterns of post-transcriptional regulators Hfq and CsrA revealed by UV crosslinking in vivo.
538 *EMBO J.* 35, 991–1011. doi:10.15252/embj.201593360.
- 539 Hommais, F., Oger-Desfeux, C., Van Gijsegem, F., Castang, S., Ligori, S., Expert, D., et al. (2008). PecS is a
540 global regulator of the symptomatic phase in the phytopathogenic bacterium *Erwinia chrysanthemi* 3937. *J*
541 *Bacteriol* 190, 7508–22. doi:10.1128/JB.00553-08.
- 542 Jahn, C. E., Selimi, D. A., Barak, J. D., and Charkowski, A. O. (2011). The *Dickeya dadantii* biofilm matrix
543 consists of cellulose nanofibres, and is an emergent property dependent upon the type III secretion system and
544 the cellulose synthesis operon. *Microbiology* 157, 2733–2744. doi:10.1099/mic.0.051003-0.

- 545 Jiang, X., Sobetzko, P., Nasser, W., Reverchon, S., and Muskhelishvili, G. (2015). Chromosomal “stress-
546 response” domains govern the spatiotemporal expression of the bacterial virulence program. *MBio* 6, e00353-
547 00315. doi:10.1128/mBio.00353-15.
- 548 Kajitani, M., Kato, A., Wada, A., Inokuchi, Y., and Ishihama, A. (1994). Regulation of the Escherichia coli
549 hfq gene encoding the host factor for phage Q beta. *J. Bacteriol.* 176, 531–534.
- 550 Kambara, T. K., Ramsey, K. M., and Dove, S. L. (2018). Pervasive Targeting of Nascent Transcripts by Hfq.
551 *Cell Rep* 23, 1543–1552. doi:10.1016/j.celrep.2018.03.134.
- 552 Kunte, H. J., Crane, R. A., Culham, D. E., Richmond, D., and Wood, J. M. (1999). Protein ProQ influences
553 osmotic activation of compatible solute transporter ProP in Escherichia coli K-12. *J. Bacteriol.* 181, 1537–
554 1543.
- 555 Lai, J.-L., Tang, D.-J., Liang, Y.-W., Zhang, R., Chen, Q., Qin, Z.-P., et al. (2018). The RNA chaperone Hfq is
556 important for the virulence, motility and stress tolerance in the phytopathogen Xanthomonas campestris.
557 *Environ Microbiol Rep.* doi:10.1111/1758-2229.12657.
- 558 Leonard, S., Hommais, F., Nasser, W., and Reverchon, S. (2017). Plant-phytopathogen interactions: bacterial
559 responses to environmental and plant stimuli: Molecular dialog between phytopathogens and plants.
560 *Environmental Microbiology* 19, 1689–1716. doi:10.1111/1462-2920.13611.
- 561 Leonard, S., Meyer, S., Lacour, S., Nasser, W., Hommais, F., and Reverchon, S. (2019). APERO: a genome-
562 wide approach for identifying bacterial small RNAs from RNA-Seq data. *Nucleic Acids Res.*
563 doi:10.1093/nar/gkz485.
- 564 Link, T. M., Valentin-Hansen, P., and Brennan, R. G. (2009). Structure of Escherichia coli Hfq bound to
565 polyriboadenylate RNA. *Proc. Natl. Acad. Sci. U.S.A.* 106, 19292–19297. doi:10.1073/pnas.0908744106.
- 566 Ma, B., Hibbing, M. E., Kim, H.-S., Reedy, R. M., Yedidia, I., Breuer, J., et al. (2007). Host range and
567 molecular phylogenies of the soft rot enterobacterial genera pectobacterium and dickeya. *Phytopathology* 97,
568 1150–1163. doi:10.1094/PHYTO-97-9-1150.
- 569 Maes, M., and Messens, E. (1992). Phenol as grinding material in RNA preparations. *Nucleic Acids Res* 20,
570 4374.
- 571 Mark Glover, J. N., Chaulk, S. G., Edwards, R. A., Arthur, D., Lu, J., and Frost, L. S. (2015). The FinO family
572 of bacterial RNA chaperones. *Plasmid* 78, 79–87. doi:10.1016/j.plasmid.2014.07.003.
- 573 Melamed, S., Adams, P. P., Zhang, A., Zhang, H., and Storz, G. (2020). RNA-RNA Interactomes of ProQ and
574 Hfq Reveal Overlapping and Competing Roles. *Molecular Cell* 77, 411-425.e7.
575 doi:10.1016/j.molcel.2019.10.022.
- 576 Meyer, S., Reverchon, S., Nasser, W., and Muskhelishvili, G. (2018). Chromosomal organization of
577 transcription: in a nutshell. *Current Genetics* 64, 555–565. doi:10.1007/s00294-017-0785-5.
- 578 Miller, J. G. (1972). Living systems: The organization. *Behavioral Science* 17, 1–182.
579 doi:10.1002/bs.3830170102.
- 580 Milner, J. L., and Wood, J. M. (1989). Insertion proQ220::Tn5 alters regulation of proline porter II, a
581 transporter of proline and glycine betaine in Escherichia coli. *J. Bacteriol.* 171, 947–951.
- 582 Moran, F., Nasuno, S., and Starr, M. P. (1968). Oligogalacturonide trans-eliminase of Erwinia carotovora.
583 *Arch. Biochem. Biophys.* 125, 734–741.

***Dickeya dadantii proQ* and *hfq* mutant characterization**

- 584 Ouafa, Z.-A., Reverchon, S., Lautier, T., Muskhelishvili, G., and Nasser, W. (2012). The nucleoid-associated
585 proteins H-NS and FIS modulate the DNA supercoiling response of the *pel* genes, the major virulence factors
586 in the plant pathogen bacterium *Dickeya dadantii*. *Nucleic Acids Research* 40, 4306–4319.
587 doi:10.1093/nar/gks014.
- 588 Prigent-Combaret, C., Zghidi-Abouzeid, O., Effantin, G., Lejeune, P., Reverchon, S., and Nasser, W. (2012).
589 The nucleoid-associated protein Fis directly modulates the synthesis of cellulose, an essential component of
590 pellicle-biofilms in the phytopathogenic bacterium *Dickeya dadantii*: *Dickeya dadantii* Fis protein and biofilm
591 formation. *Molecular Microbiology* 86, 172–186. doi:10.1111/j.1365-2958.2012.08182.x.
- 592 R Core Team (2020). R: A language and environment for statistical computing. R Foundation for Statistical
593 Computing, Vienna, Austria. URL <https://www.R-project.org/>.
- 594 Reverchon, S., Meyer, S., Forquet, R., Hommais, F., Muskhelishvili, G., and Nasser, W. (2021). The nucleoid-
595 associated protein IHF acts as a “transcriptional domainin” protein coordinating the bacterial virulence traits
596 with global transcription. *Nucleic Acids Res* 49, 776–790. doi:10.1093/nar/gkaa1227.
- 597 Reverchon, S., and Nasser, W. (2013). *Dickeya* ecology, environment sensing and regulation of virulence
598 programme. *Environ Microbiol Rep* 5, 622–636. doi:10.1111/1758-2229.12073.
- 599 Roeder, D. L., and Collmer, A. (1985). Marker-exchange mutagenesis of a pectate lyase isozyme gene in
600 *Erwinia chrysanthemi*. *J. Bacteriol.* 164, 51–56.
- 601 Sheidy, D. T., and Zielke, R. A. (2013). Analysis and Expansion of the Role of the *Escherichia coli* Protein
602 ProQ. *PLoS ONE* 8, e79656. doi:10.1371/journal.pone.0079656.
- 603 Smirnov, A., Förstner, K. U., Holmqvist, E., Otto, A., Günster, R., Becher, D., et al. (2016). Grad-seq guides
604 the discovery of ProQ as a major small RNA-binding protein. *Proc. Natl. Acad. Sci. U.S.A.* 113, 11591–11596.
605 doi:10.1073/pnas.1609981113.
- 606 Smirnov, A., Wang, C., Drewry, L. L., and Vogel, J. (2017). Molecular mechanism of mRNA repression in
607 *trans* by a ProQ-dependent small RNA. *The EMBO Journal* 36, 1029–1045. doi:10.15252/embj.201696127.
- 608 Sobrero, P., and Valverde, C. (2012). The bacterial protein Hfq: much more than a mere RNA-binding factor.
609 *Crit. Rev. Microbiol.* 38, 276–299. doi:10.3109/1040841X.2012.664540.
- 610 Teather, R. M., and Wood, P. J. (1982). Use of Congo red-polysaccharide interactions in enumeration and
611 characterization of cellulolytic bacteria from the bovine rumen. *Appl. Environ. Microbiol.* 43, 777–780.
- 612 Toth, I., van der Wolf, J. M., Sadtler, G., Lojkowska, E., Hélias, V., Pirhonen, M., et al. (2011). *Dickeya*
613 species: an emerging problem for potato production in Europe. *Plant Pathology* 60, 385–399.
- 614 Tsui, H. C., and Winkler, M. E. (1994). Transcriptional patterns of the *mutL-miaA* superoperon of *Escherichia*
615 *coli* K-12 suggest a model for posttranscriptional regulation. *Biochimie* 76, 1168–1177.
- 616 Updegrove, T. B., Zhang, A., and Storz, G. (2016). Hfq: the flexible RNA matchmaker. *Current Opinion in*
617 *Microbiology* 30, 133–138. doi:10.1016/j.mib.2016.02.003.
- 618 Vogel, J., and Luisi, B. F. (2011). Hfq and its constellation of RNA. *Nat. Rev. Microbiol.* 9, 578–589.
619 doi:10.1038/nrmicro2615.
- 620 Wagner, E. G. H. (2013). Cycling of RNAs on Hfq. *RNA Biology* 10, 619–626. doi:10.4161/rna.24044.
- 621 Wang, C., Pu, T., Lou, W., Wang, Y., Gao, Z., Hu, B., et al. (2018). Hfq, a RNA Chaperone, Contributes to

- 622 Virulence by Regulating Plant Cell Wall-Degrading Enzyme Production, Type VI Secretion System
623 Expression, Bacterial Competition, and Suppressing Host Defense Response in *Pectobacterium carotovorum*.
624 *Mol. Plant Microbe Interact.*, MPMI12170303R. doi:10.1094/MPMI-12-17-0303-R.
- 625 Westermann, A. J., Venturini, E., Sellin, M. E., Förstner, K. U., Hardt, W.-D., and Vogel, J. (2019). The Major
626 RNA-Binding Protein ProQ Impacts Virulence Gene Expression in *Salmonella enterica* Serovar Typhimurium.
627 *mBio* 10. doi:10.1128/mBio.02504-18.
- 628 Wilms, I., Möller, P., Stock, A.-M., Gurski, R., Lai, E.-M., and Narberhaus, F. (2012). Hfq influences multiple
629 transport systems and virulence in the plant pathogen *Agrobacterium tumefaciens*. *J. Bacteriol.* 194, 5209–
630 5217. doi:10.1128/JB.00510-12.
- 631 Zeng, Q., McNally, R. R., and Sundin, G. W. (2013). Global small RNA chaperone Hfq and regulatory small
632 RNAs are important virulence regulators in *Erwinia amylovora*. *J. Bacteriol.* 195, 1706–1717.
633 doi:10.1128/JB.02056-12.

634

635 **9 Supplementary Material**

636 Table S1 to S4 in file named SupplementaryMaterials_Leonard.pdf

637 Figures S1 to S5 in file named SupplementaryMaterials_Leonard.pdf